



ORIGINAL ARTICLE

Non-enzymatic colorimetric biosensor for hydrogen peroxide using lignin-based silver nanoparticles tuned with ionic liquid as a peroxidase mimic



Umar Nishan^{a,*}, Aatif Niaz^a, Nawshad Muhammad^b, Muhammad Asad^a,
Azhar-ul-Haq Ali Shah^a, Naeem Khan^a, Mansoor Khan^a, Shaukat Shujah^a,
Abdur Rahim^{c,*}

^a Department of Chemistry, Kohat University of Science and Technology, Kohat 26000, KPK, Pakistan

^b Department of Dental Materials, Institute of Basic Medical Sciences Khyber Medical University, Peshawar, KPK, Pakistan

^c Interdisciplinary Research Centre in Biomedical Materials (IRCBM), COMSATS University Islamabad, Lahore Campus 54000, Pakistan

Received 1 March 2021; accepted 12 April 2021

Available online 21 April 2021

KEYWORDS

Lignin mediated synthesis;
Ionic liquid;
Silver NPs;
Colorimetric sensor;
Hydrogen peroxide;
Peroxidase mimic

Abstract Hydrogen peroxide (H₂O₂) is a byproduct of oxidative metabolism, acts as a signaling molecule, and can induce protein and DNA damage by oxidative stress. Ionic liquid-coated lignin stabilized silver nanoparticles (LAGNPs) have been used for the colorimetric detection of H₂O₂. Both ionic liquid and lignin moieties have a synergistic effect on the conductivity of silver nanoparticles to display intrinsic peroxidase-like activity with the enhanced potential to catalyze the oxidation of substrate 3,3',5,5'-tetramethylbenzidine (TMB). LAGNPs have been synthesized by the green synthesis method and the prepared nanoparticles have been characterized by different techniques such as FTIR, EDX, TGA, SEM, and XRD. 1-H-3-methylimidazolium acetate (ionic liquid) was prepared and used for tuning of AgNPs. By using ionic liquid capped LAGNPs the colorimetric detection of H₂O₂ was done with the assistance of TMB solution and results were analyzed by UV-Vis spectrophotometer. Different parameters such as (amount of capping agent and TMB, pH, H₂O₂ concentration, and time) were optimized to get the best results of the proposed sensor. The H₂O₂ biosensor exhibited a linear response in the range of 1×10^{-9} – 3.6×10^{-7} M, with a detection limit of 1.379×10^{-8} M and a quantification limit of 4.59×10^{-8} M, and R² of 0.999. The sensor gave a short response time of 5 min for colorimetric detection of H₂O₂ at pH 7.5 and room temperature. For the detection of hydrogen peroxide, the proposed sensor showed good sen-

* Corresponding authors at: Department of Chemistry, Kohat University of Science and Technology (KUST), Kohat, KPK, Pakistan.
E-mail addresses: umarnishan85@gmail.com (U. Nishan), rahimkhan533@gmail.com (A. Rahim).

Peer review under responsibility of King Saud University.



sitivity and selectivity and was successfully employed for the detection of H_2O_2 in the blood serum samples of hypertension patients.

© 2021 The Author(s). Published by Elsevier B.V. on behalf of King Saud University. This is an open access article under the CC BY-NC-ND license (<http://creativecommons.org/licenses/by-nc-nd/4.0/>).

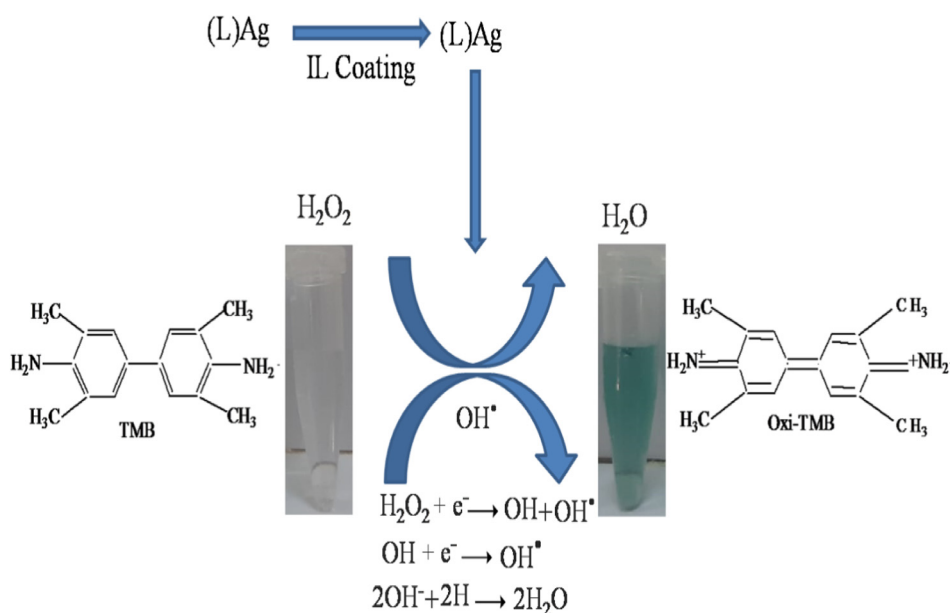
1. Introduction

Hydrogen peroxide (H_2O_2) is formed as a byproduct of oxidative metabolism. In the biological system, peroxidases play important role in the catalytic degradation of H_2O_2 (Wang et al., 2015). The concentration of hydrogen peroxide is regulated by peroxidases, which are generally generated from human red blood cells and kidneys (Kirkman and Gaetani, 2007). The concentration of hydrogen peroxide is regulated through peroxidases but for their functioning, they still need ambient conditions of temperature and pH, etc. (Favre et al., 2011). The monitoring of hydrogen peroxide is also critical in many other fields such as biological processes, paper bleaching, chemical, sterilization processes, pulp, clinical and food production, etc- H_2O_2 also plays an important role in food security, environmental protection as well as in bioanalysis (Nossol and Zarbin, 2009) therefore, it is also important to monitor the concentration of hydrogen peroxide (Salimi et al., 2007). To monitor, the concentration of hydrogen peroxide is also possible through multiple routes. The determination of hydrogen peroxide can be done through enzymatic methods (Tian et al., 2013). Due to certain limitations of the enzymatic methods such as low shelf life, high cost, less stability, difficult transportation, and delicate handling enzymatic sensing of the analyte become undesirable. On the other hand, nanomaterials-based detection is gaining more interest owing to its cost-effectiveness, ease in preparations, stability, and easy transportation (Tian et al., 2013) (see Scheme 1).

Various sophisticated techniques have been utilized for the determination of hydrogen peroxide such as chromatographic (Nakashima et al., 1994), spectrophotometric (Lu et al., 2016), chemiluminescence (Haddad Irani-nezhad et al., 2019), and electrochemical methods (Chen et al., 2014; Theyagarajan et al., 2020). Compared with other techniques colorimetric method is low cost, highly sensitive, and selective for hydrogen peroxide determination (Wang et al., 2016; Chen et al., 2016). Colorimetric analysis is commonly used for field analysis and point-of-care diagnosis owing to its efficiency, simple operation, and sensitivity (Liu et al., 2012).

Over the last few years, researchers have been focused on the synthesis of metal nanoparticles and their application because of their novel properties such as optical, electronic, magnetic, thermal, sensor devices, and catalysis, etc (Daniel and Astruc, 2004; Schmid et al., 2004). According to literature the monitoring of hydrogen peroxide has become more important due to its wide applications such as food industries, textile paper, and cleaning products. Hydrogen peroxide is a powerful oxidizing agent as well as its derivatives, which can be employed to treat environmental pollutants such as aldehydes, chlorine, phenols, and other aromatic compounds and also used in the synthesis of many organic compounds (Usui et al., 2003; Hasebe and Eguchi, 2003). As several enzymatic reactions produce H_2O_2 as an end product, its concentration can be used as a measure of the progress of a reaction (Jiang and Miles, 1993).

For the preparation and stabilization of nanoparticles, ionic liquids (ILs) have been explored as excellent media for



Scheme 1 Proposed reaction mechanism for the detection of H_2O_2 .

their applications (Wang et al., 2015). Although ILs are solvents for different nanomaterials due to their low vapor pressure and a wide range of stable temperatures (Rogers and Seddon, 2003; Wang and Hao, 2016). Capping of nanomaterials with ionic liquid is used to get catalytic reactions that are not possible with the help of other solvents because IL prevents the nanomaterials from aggregations and enhances the electrical conductivity as recently reported by our group (Nishan et al., 2019; Nishan et al., 2021).

Due to their large surface-to-volume ratio, high catalytic performance, structure-dependent properties, and tunable optical properties, nanoparticles have received significant attention over the last few years. (Wen et al., 2008). According to the literature, different materials have been used as peroxidase mimics for H₂O₂ detection, including metal oxide and magnetic nanoparticles, conjugated polymers, bimetallic alloy nanoparticles, carbon nanotubes, and noble metal nanoparticles (He et al., 2017; Xie et al., 2018; Shin et al., 2017).

In the present work, silver nanoparticles were prepared by using lignin as stabilizing and reducing agent, furthermore a conductive layer of lignin was obtained on the surface of the AgNPs (Chen et al., 2017). The LAgNPs were characterized by diverse techniques like FTIR, SEM, TGA, EDX, and XRD. After characterization LAgNPs were capped/tuned with ionic liquid (1-H-3-methylimidazolium acetate) to further enhance the catalytic activity, stability, and conductivity, and dispersibility in comparison to other peroxidase mimics for the colorimetric detection of hydrogen peroxide. The proposed material LAgNPs was used as promising peroxidase mimics for the colorimetric determination of H₂O₂. To achieve the optimum performance of the IL capped lignin-based silver nanoparticles, different parameters have been optimized, such as (a) pH (b) amount of LAg/IL (c) incubation period (d) TMB and (e) H₂O₂ concentration. The proposed sensor was applied for the determination of hydrogen peroxide in the real samples (in hypertension patient's blood).

2. Materials and methods

2.1. Reagents and materials

All the chemicals used were of analytical grade: silver nitrate, 3,3',5,5'-tetramethylbenzidine (TMB), acetic acid CH₃COOH (99.9%), and sodium borohydride (NaBH₄) were purchased from Sigma-Aldrich. Hydrogen peroxide (H₂O₂, 35%) was obtained from Merck KGaA. 1-methylimidazole C₄H₆N₂ (99.2%) was purchased from ACROS. The saline phosphate buffer (PBS, pH-7.4) was acquired from Bio World. Cuvettes (Disposable) with 2 mL of volume capacity were purchased from Kartell. Without further purification, all chemicals were used and they were of analytical grade. Deionized water was utilized for the preparation of the different solutions.

2.2. Instrumentation

The characteristic peaks were recorded on UV-Vis double beam spectrophotometer (Shimadzu, UV-1800, Germany) using quartz cuvettes. Functional groups of the prepared NPs were investigated by using FTIR MX-300 (USA). The size and morphology of the synthesized nanoparticles were evalu-

ated by using SEM (JSM-5910, Japan) and elemental analysis was performed on EDX equipped with SEM. The crystal structure of the prepared nanoparticles was studied by using XRD Bruker Smart Apex CCD. On a Perkin-Elmer STA 6000 thermal analyzer with a heating rate of 10 °C/min in a temperature range from 30 to 800 °C under the nitrogen atmosphere, thermogravimetric analysis (TGA) was carried out. The Raman spectrum of the prepared nanoparticles were recorded at room temperature using a portable Raman instrument (i-Raman, Bwtek Inc., U.S.A.) attached with a microscope (20X objectives).

2.3. Synthesis of lignin doped silver nanoparticles

For the synthesis of Lignin Doped Ag NPs, 50 mL of Longan fruit (Dimocarpus longan Lour) was prepared in 100 mL double-distilled water. The obtained extract of longan juice was added dropwise to 50 mM solution of lignin and 50 mM solution of AgNO₃. The reaction mixture was magnetically stirred for 3 h at room temperature and the solution was stored at 5 °C for 24 h. Lignin doped Ag nanoparticles were then separated by centrifugation at 800 rpm for 10 min at room temperature and were collected in the pellet. After that, the prepared nanoparticles were dried in an oven at 40 °C as shown in Fig. 1 (A). The nanoparticles were stored at room temperature in an Eppendorf tube for further use. The reproducibility of the process was confirmed by repeating the synthesis of the nanoparticles to get a good amount for different experiments.

2.4. Capping of lignin doped silver nanoparticles with ionic liquid

The ionic liquid synthesis was carried out according to the protocol earlier reported by our group (Nishan et al., 2020). Lignin-doped silver nanoparticles dispersion was done in ionic liquid. To achieve the desired dispersion, 3 mL of ionic liquid (1-H-3-methylimidazolium acetate) was taken via a micro pipette in a china dish and 18 mg of silver nanoparticles doped with lignin were taken and then applied to the ionic liquid. Maceration of the nanoparticles and the ionic liquid was done for around 20 min with the aid of the pestle and mortar as shown in Fig. 1(C). A greyish mixture of lignin-doped Ag NPs with ionic liquid was collected and the mixture was placed for further use in an Eppendorf tube.

2.5. Colorimetric detection of hydrogen peroxide

Hydrogen peroxide and TMB solutions were prepared in deionized water. 30 μL ionic liquid capped lignin doped silver nanoparticles were taken and then 100 μL of hydrogen peroxide solution (3.6 × 10⁻⁷ M) was added into the ionic liquid coated lignin doped silver nanoparticles followed by the addition of PBS solution. The reaction was done at room temperature. By increasing concentrations of H₂O₂, the colorimetric change was observed and the color change from transparent to a greenish color, and the spectrum of absorption was captured by UV-Vis spectrophotometer. The detection performance of the proposed sensor was evaluated with respect to ionic liquid coated lignin doped silver nanoparticles, H₂O₂ concentration, TMB, pH, and buffer solution concentration.

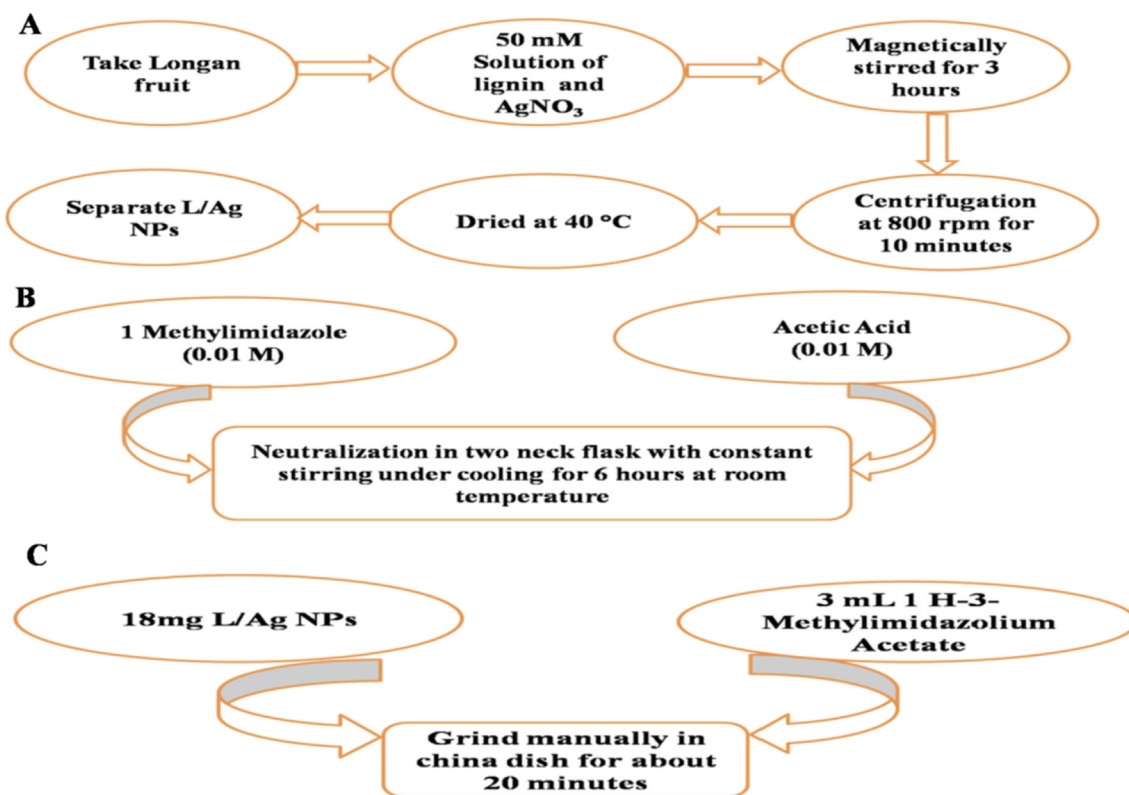


Fig. 1 (A) Synthesis of Lignin doped silver nanoparticles (B) Synthesis of ionic liquid (C) Capping of Lignin doped silver nanoparticles with ionic liquid.

3. Results and discussions

3.1. Characterization of the lignin doped silver nanostructures

3.1.1. FTIR analysis of the prepared nanoparticles

The FTIR spectrum of the prepared nanoparticles is shown in Fig. 2. The possible biomolecules take part in the stabilization and capping of the lignin doped silver NPs synthesized by Longan fruit juice. The FTIR spectrum displays absorption bands at 3365, 2911, 1633, 1521, and 1035 cm^{-1} as shown in Fig. 2. The 3370 cm^{-1} and 2911 cm^{-1} absorption bands reflect

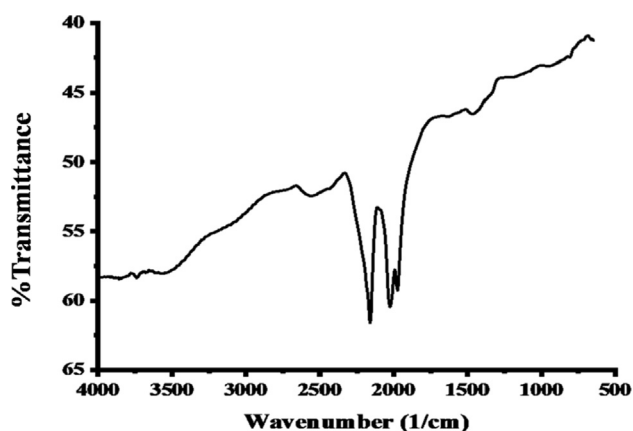


Fig. 2 FTIR spectrum of L/AgNPs.

stretching of hydrogen-bonded-OH and vibration of sp² C—H (alkane) respectively. N—H bend vibration can be attributed to the absorption at 1521 cm^{-1} and the peak at 1633 cm^{-1} can be attributed to the C—C symmetric stretching vibration of aromatic rings. The band might be contributed by the C—N bonds at 1035 cm^{-1} . It is evident from the FTIR spectrum that the OH group is present in Lignin juice, which is responsible for reducing silver ions to silver nanoparticles (Badiya and Ramamurthy, 2018).

3.1.2. The synthesized nanostructures' XRD pattern

The XRD spectrum of the nanoparticles prepared is shown in Fig. 3. X-ray diffraction analysis at 20–80° confirmed the crystalline structure of lignin-doped silver nanoparticles. Different

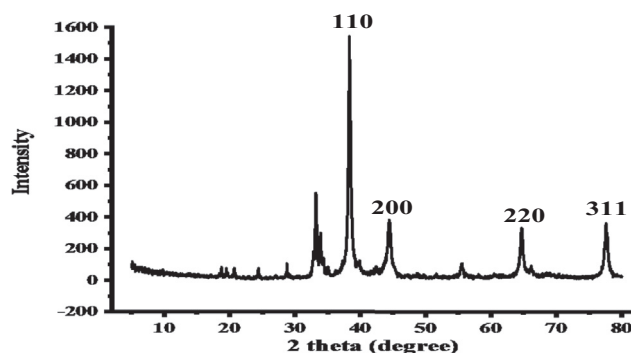


Fig. 3 XRD pattern of L/AgNPs.

numbers of lattice planes represented at (111), (200), (220) and (311) and different numbers of Bragg's reflection with 2 theta values at 38.31°, 44.44°, 64.7°, and 77° show that the prepared nanoparticles have faced centered cubic structure (Zhang et al., 2019). All the peaks are in good agreement with JCPDS file number 00-004-0783. XRD spectrum show strong diffraction peaks at 38.31°, 44.44°, and 64.7°. The peak that corresponds to (110) is more prominent than the other planes, implying that the dominant orientation is (110).

The average particle size of the prepared lignin-doped silver nanoparticles was calculated through the Scherrer equation on the face center cubic phase.

$$D = K\lambda/\beta\cos\theta$$

K = coefficient (0.89) and θ represent the angle of diffraction at the maximum peak.

D = crystal size of the catalyst,

λ = X-ray wavelength,

β = full width at half maximum (FWHM) of the diffraction peak (radian),

The average crystal size of face center cubic phase lignin doped silver NPs were calculated to be ~ 30 nm.

3.1.3. SEM analysis of the nanostructures prepared

Fig. 4 demonstrates the morphology of lignin doped silver nanoparticles was characterized by Scanning Electron Microscopy (SEM). SEM is used to characterize the surface morphology, particle shape, and size (Asnis, 2018). The SEM image shows that the synthesized lignin doped nanoparticles are granular agglomerated cluster structures owing to the strong tendency of agglomeration.

3.1.4. EDX analysis of lignin doped silver NPs

Fig. 5 demonstrates the chemical composition of lignin-doped silver NPs that have been examined by EDX analysis. This confirmed the existence of silver and oxygen in the sample of prepared nanoparticles (Hoyo et al., 2020). The silver and oxygen content by EDX analysis were found to be 87.84 and 12.16% by weight, respectively as shown in Table 1.

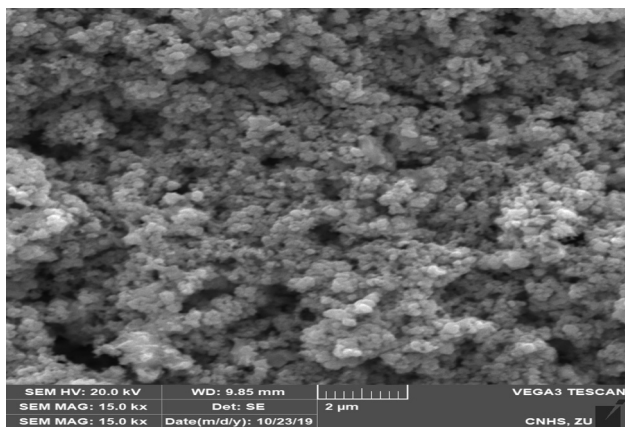


Fig. 4 SEM image of the prepared L/AgNPs, magnification of 15 kx.

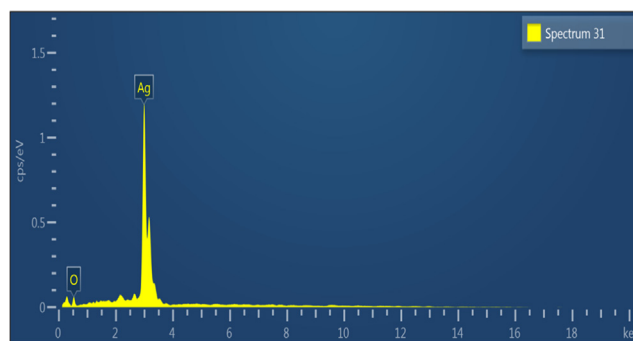


Fig. 5 EDX spectrum of the synthesized L/AgNPs.

3.1.5. Thermal gravimetric assessment of the nanoparticles prepared

Fig. 6 demonstrates that the prepared lignin-doped silver NPs were analyzed by thermogravimetric analysis (TGA). The thermal stability of the lignin-doped silver NPs is shown in Fig. 5. To investigate the combustion properties of the prepared nanoparticles TGA-Q5000 apparatus (TA Co., USA) was used from 50 to 800 °C at a heating rate of 10 °C min⁻¹. From the TGA curve, it is observed that the weight loss of the nanoparticles occurred in the 50 to 800 °C temperature range. The weight of all samples was maintained within 2–4 mg in an open platinum pan (Shankar and Rhim, 2017).

3.2. Colorimetric detection of hydrogen peroxide

For the colorimetric detection of hydrogen peroxide, a simple assay was designed as shown in Fig. 7. For the sensing of hydrogen peroxide, ionic liquid capped lignin doped silver nanoparticles (30 μ L) were used. TMB solution 180 μ L (10 mM) and PBS solution 550 μ L (6 mM) was mixed with 100 μ L hydrogen peroxide solution (3.6×10^{-7} M). After the addition of hydrogen peroxide solution to the capped lignin doped silver nanoparticles, the color changes from transparent to greenish. The UV-Vis spectrum and the colorimetric change can be seen in Fig. 7.

3.3. Proposed mechanism of hydrogen peroxide detection

The peroxidase-like activity of ionic liquid capped lignin doped silver nanoparticles was confirmed from the catalytic oxidation of a 3,3',5,5'-Tetramethylbenzidine (TMB) by H₂O₂ to form a bluish-green product. Their absorbance was also recorded by UV-Vis spectrophotometer, which demonstrates a broad peak at 653 nm for the oxidized TMB. The mechanism of the proposed reaction is as follows; Ionic liquid capped lignin doped silver nanoparticles absorb photon (light) whose energy is equal to its bandgap energy. Due to this absorption of photon excitation of electron takes place from the valence band to conduction band to yield electrons and H⁺ pair. After this H₂O₂ having a strong oxidation ability to scavenge the excited electron to prevent the recombination of the electron and H⁺ and generate OH radicals and OH⁻ ions. Moreover, hydrogen peroxide adsorbs on the surface of ionic liquid capped lignin doped silver nanoparticles to form peroxy complex between Ag and H₂O₂ that enhance the absorption capability of ionic liquid capped lignin doped silver nanoparticles under visible

Table 1 EDX analysis.

Element	Line Type	Weight %	Weight % Sigma	Atomic %
Ag	L series	87.84	1.89	51.72
O	K series	12.16	1.89	48.28
Total		100.00		100.00

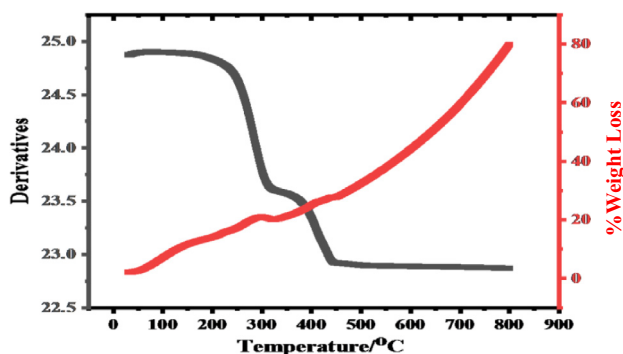
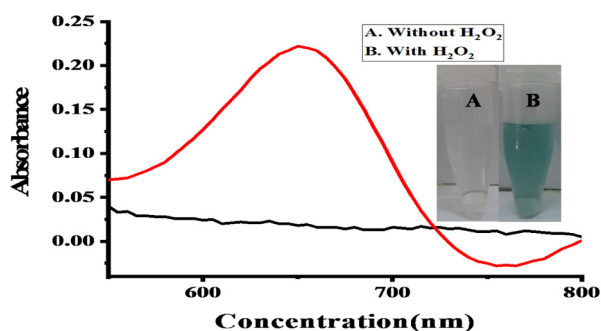
**Fig. 6** TGA curves of the synthesized L/AgNPs.

Fig. 7 Shows the UV-Vis spectra and the colorimetric change. The colorimetric change was observed with a solution containing 30 μL ionic liquid capped nanoparticles, 180 μL TMB solution (10 mM), 550 μL buffer solution (6 mM), and 100 μL hydrogen peroxide solution (3.6×10^{-7} M). (A) In the absence of hydrogen peroxide (B) in the presence of 100 μL hydrogen peroxide solution (3.6×10^{-7} M), the color changes from transparent to greenish.

light. As a result, more OH radicals are formed that lead to increasing TMB oxidation to form blue-green products as shown in equation 3 (Velegraki et al., 2006).

3.4. Optimization-of the method proposed

3.4.1. Effect of capping amount

The optimization of ionic liquid-coated nanostructures is shown in Fig. 8(A). The colorimetric detection of H_2O_2 , the peroxidase-like activity was evaluated using TMB as a substrate. The reaction was carried out as follow; 30 μL of IL coated NPs, 180 μL of TMB solution (10 mM), 550 μL of phosphate-buffer solution (6 mM), and 100 μL H_2O_2 solution having concentration (3.6×10^{-7} M). The reaction was incubated for 5 min to detect the colorimetric change. 30 μL ionic

liquid capped lignin doped silver nanoparticles are compatible with 100 μL hydrogen peroxide (3.6×10^{-7} M). In short 30 μL , the capped amount is optimum at which the color completely changes from transparent to greenish. In 2018, Zarif et al. reported that 35 μL IL coated iron NPs were the optimum amount for H_2O_2 detection (Zarif et al., 2018). The quantitative relationship between IL-coated NPs, TMB, and varying concentrations of hydrogen peroxide was also recorded by UV-Vis spectroscopy as revealed in Fig. 8(A).

3.4.2. Effect of pH on the response of the sensor

Fig. 8 (B) shows the optimization of pH for the proposed reaction. With different pH values of pH 3–11, the response of the proposed sensor was optimized. The pH optimization was performed by using sodium hydroxide and hydrochloric acid solutions. The best colorimetric change of the proposed sensor occurred at the following optimum conditions; 30 μL IL-based lignin doped silver nanoparticles, 180 μL TMB solution (10 mM), pH 7.5, incubation time 5 min, and 100 μL hydrogen peroxide (3.6×10^{-7} M). By increasing the concentration of H_2O_2 the best colorimetric change of our proposed sensor occurred at pH 7.5. So the pH 7.5 was selected as optimum for the proposed sensor. According to the literature, the optimal pH for the proposed sensor was reported to be 7.4 (Zarif et al., 2020).

3.4.3. Effect of TMB on the sensor

Fig. 8(C) shows the optimization of the TMB solution. By using TMB as a substrate the peroxidase-like properties of the synthesized lignin doped silver nanoparticles were evaluated. Fig. 8(C) demonstrate that when 100 μL H_2O_2 solution having concentration (3.6×10^{-7} M) is added to 30 μL capped nanoparticles, 180 μL TMB (10 mM) and 550 μL of phosphate-buffer solution (6 mM) together, the color change from colorless to bluish-green, and the absorbance was also recorded through UV-Vis spectrum at 652 nm. Thus the TMB solution having a concentration of 10 mM (180 μL) was selected optimum for the proposed sensor. While in literature 0.5 mM concentration of TMB solution was reported (Zhang et al., 2018). In the absence of TMB, the reaction of H_2O_2 , and lignin doped silver NPs does not occur. This phenomenon shows that the intrinsic peroxidase-like activity of the synthesized lignin-doped silver nanoparticles, similar to other noble metal-based peroxidase mimics.

3.4.4. Time impact on sensitivity

The time optimization study was conducted in the range of (1–10 min) as shown in Fig. 8(D). The proposed sensor LAgNPs gave the best response at a time of 5 min because maximum conversion (oxidation) occurred at this time. Thus 5 min was

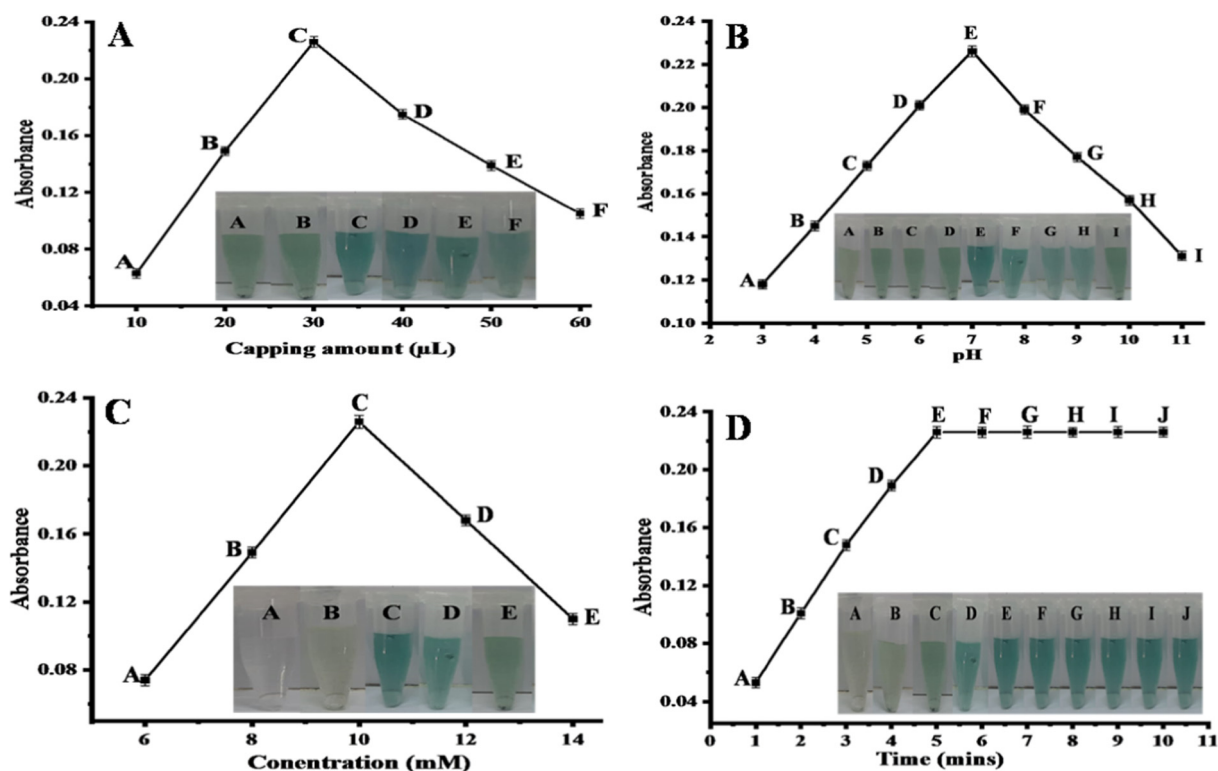


Fig. 8 (A) The effect of capping amount (μL). The best colorimetric change was observed at 30 μL capped nanoparticles, 180 μL TMB solution (10 mM), 550 μL buffer solution (6 mM), and 100 μL H_2O_2 solution (3.6×10^{-7} M). (B) Optimization of pH in the range of pH (3–11), under optimized conditions: 30 μL capped nanoparticles, 180 μL TMB solution (10 mM), 550 μL buffer solution (6 mM) and 100 μL H_2O_2 solution (3.6×10^{-7} M). (C) Optimization of the TMB solution under optimized conditions: 30 μL capped nanoparticles, 180 μL TMB solution (6–14 mM), 550 μL buffer solution (6 mM), and 100 μL H_2O_2 solution (3.6×10^{-7} M). (D) Time optimization (1–10 min), under optimized conditions: 30 μL capped nanoparticles, 180 μL TMB solution (10 mM), 550 μL buffer solution (6 mM), and 100 μL H_2O_2 solution (3.6×10^{-7} M).

chosen as the optimal time for the colorimetric detection of H_2O_2 . In the case of the reported sensor (Zhang et al., 2019), however, the optimum time for the reported sensor was 30 min. Our proposed sensor showed a rapid detection of H_2O_2 compared to the already published literature.

3.4.5. Analytical specifications of the proposed sensor

The analytical features of the proposed sensor for hydrogen peroxide concentration were evaluated by applying a calibration graph. As shown in Fig. 9(A), the optimization was achieved with various concentrations of hydrogen peroxide. The peroxidase-like activity of IL coated lignin doped silver nanoparticles under the optimum experimental condition was conducted for colorimetric detection of hydrogen peroxide. It can be observed that by rising the concentration of hydrogen peroxide the UV–Vis spectrum shows a peak at 652 nm that increases linearly with the rise in hydrogen peroxide concentration as shown in Fig. 9(A). The proposed sensor showed a linear response to hydrogen peroxide in the range of 1×10^{-9} – 3.6×10^{-7} M, with a LOD of 1.37×10^{-8} M and LOQ 4.59×10^{-8} M, with an R^2 value of 0.999. By using the formulas ($10\sigma/\text{slope}$) for LOQ and ($3\sigma/\text{slope}$) for LOD the values were calculated. The σ represents the standard deviation of the blank and the slope value is derived from the linear curve. By comparing the proposed sensor results with the reported literature (Lin et al., 2015), the limit of detection

($5.3 \mu\text{M}$) is low and the R^2 value is 0.994. Fig. 9 (B) demonstrates the linear curve obtained with different concentrations (1×10^{-9} – 3.6×10^{-7} M) of H_2O_2 as a function of absorbance (nm), calculated at 652 nm to detect the strong optical changes as shown in Fig. 9 (A). Compared with the literature already published, Table 2 shows the analytical efficiency of the proposed sensor (Wang et al., 2016; Nguyen et al., 2018; Choleva et al., 2018; Ding et al., 2016; Zhong et al., 2016; Xiang et al., 2016; Liu et al., 2015).

3.5. Interference studies

The selectivity of the proposed sensor (IL coated lignin doped silver nanoparticles) was explored for the selective detection of hydrogen peroxide in the presence of the co-existing species. In the presence of chemicals that usually co-exist, such as ascorbic acid, urea, Ca^+ , K^+ , and folic acid, the absorbance responses of the proposed sensor were investigated as shown in Fig. 10. It demonstrates that the absorbance value of hydrogen peroxide is very high as compared to the absorbance value of ascorbic acid, urea, Ca^+ , K^+ and folic acid. By increasing the H_2O_2 concentration the absorbance spectra increase at 652 nm even in the presence of 3-fold of co-existing species, and no obvious change in absorbance was observed. The experiments were carried out in the same experimental circumstances by retaining the 3-fold concentration (1.0×10^{-6} M) of co-existing species

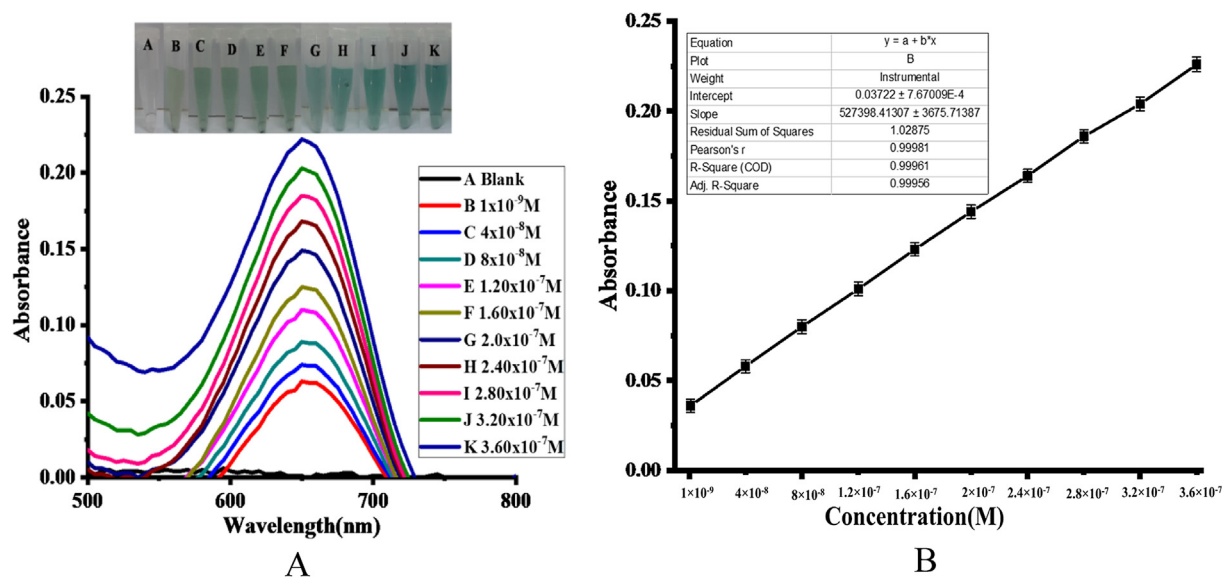


Fig. 9 (A). Colorimetric change concerning different concentrations of hydrogen peroxide and UV-Vis spectra; (B) Calibration plot of hydrogen peroxide concentration (1×10^{-9} – 3.6×10^{-7} M) versus absorbance.

Table 2 Overview of the analytical performance of the recently reported nanomaterials-based sensors for the colorimetric detection of hydrogen peroxide.

S. No	Materials used	Method applied	Limit of detection (μM)	Linear range (μM)	Ref
1	AgNPs/GQDs	Colorimetric	0.162	0.5–50	(Nguyen et al., 2018)
2	RhNPs	Colorimetric	0.75	5–125	(Choleva et al., 2018)
3	$\text{Fe}_2(\text{MoO}_4)_3\text{-F}$	Colorimetric	0.7	1–30	(Wang et al., 2016)
4	$\text{Fe}_3\text{S}_4\text{-MNPs}$	Colorimetric	0.16	2–100	(Ding et al., 2016)
5	$\beta\text{-CD/Cu-NCsa}$	Colorimetric	0.2	0.02–10	(Zhong et al., 2016)
6	AgVO ₃ nanobelts	Colorimetric	5	75–500	(Xiang et al., 2016)
7	NiO NPs	Colorimetric	8	20–100	(Liu et al., 2015)
8	NiFe LDH	Colorimetric	4.4	10–500	(Zhan et al., 2018)
9	NiSnanocubes	Colorimetric	1.72	4–40	(Liu et al., 2019)
10	Lignin Doped AgNPs	Colorimetric	0.013	0.001–0.36	Present work

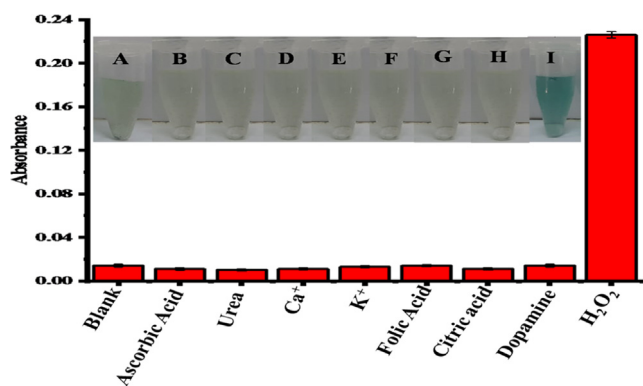


Fig. 10 Shows the interference study of hydrogen peroxide (3.6×10^{-7} M) with other analytes such as ascorbic acid, urea, Ca^+ , K^+ , and folic acid having concentration 1.0×10^{-6} M.

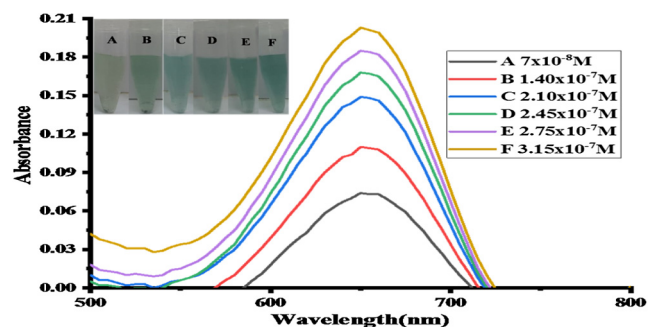


Fig. 11 shows the UV-Vis spectra of the real samples of blood serum at optimized conditions by the addition of different concentrations of hydrogen peroxide (7×10^{-8} – 3.15×10^{-7} M).

Table 3 Sensing of H₂O₂ in blood serum samples (n = 6).

Samples	Detected (nm)	H ₂ O ₂ added (nm)	H ₂ O ₂ found (nm)	Recovery (%)	RSD (%)
1	1	69	70	101.44	0.838
2	3	137	140	102.18	1.009
3	2	208	210	100.96	0.459
4	4	241	245	101.65	0.923
5	1	274	275	100.36	1.203
6	5	310	315	101.61	1.101

as compared to hydrogen peroxide (3.6×10^{-7} M). It is confirmed from these findings that, in the presence of commonly co-existing species, the sensor proposed is highly selective and precise for the detection of hydrogen peroxide. While in the case of reported literature the selectivity of the stated method for hydrogen peroxide detection, the effects of various interfering species, such as galactose, ascorbic acid, uric acid, and citric acid (Zn^{2+} , Ni^{2+} , Co^{2+} , Na^+ , Fe^{3+} , Hg^{2+}) have been examined. It was noted that the species described had no detectable effect on the detection of hydrogen peroxide up to 1 mM concentration (Swaidan et al., 2020).

3.6. Real samples analysis

The proposed sensor is applied to confirm the detection of H₂O₂ in real samples. The detection of H₂O₂ was conducted in hypertension patient's blood serum samples under the optimum experimental conditions. By using the standard addition method different concentrations of H₂O₂ such as 69, 137, 208, 241, 274, and 310 nM were spiked into the blood serum samples of hypertension patients as shown in Fig. 11. The present amount of H₂O₂ in blood serum samples solution is determined from an already established calibration plot, by using different concentrations of H₂O₂ under the same optimized condition generated at 652 nm (Swaidan et al., 2020). The percentage recovery formula is applied and the obtained results are summarized in Table 3.

$$\text{Recovery \%} = \text{H}_2\text{O}_2 \text{ found}/\text{H}_2\text{O}_2 \text{ added} \times 100$$

4. Conclusions

We report a simple method for the colorimetric detection of hydrogen peroxide based on IL capped lignin stabilized silver nanoparticles. The synthesized material lignin stabilized silver nanoparticles were confirmed through different characterization techniques. The designed protocol having ionic liquid coated nanoparticles (IL-NPs) along with 3,3',5,5'-tetramethyl benzidine (TMB) solution and buffer solution to introduce colorimetric hydrogen peroxide sensor. Under optimized conditions, the proposed sensor showed good applicability with a wide linear range (1×10^{-9} – 3.6×10^{-7} M), low limit of detection 1.37×10^{-8} M and limit of quantification 4.59×10^{-8} M with an R² value of 0.999. The proposed sensing probe is a simple, rapid, highly sensitive, selective stable biomimetic catalyst method for the colorimetric sensing of H₂O₂ that can be applied in medical diagnostics. The proposed sensor was employed for the selective detection of hydrogen peroxide in the presence of co-existing species. Furthermore, it was suc-

cessfully applied for the detection of H₂O₂ in the real samples (blood serum of hypertension patients).

Declaration of Competing Interest

The authors declare that they have no known competing financial interests or personal relationships that could have appeared to influence the work reported in this paper.

References

- Asnis, J., 2018. Production, characterization, and biodistribution of lignin-capped silver nanoparticles to combat multidrug resistant bacteria in vitro and in vivo. University of British Columbia.
- Badiya, P.K., Ramamurthy, S.S., 2018. Smartphone plasmonics for doxycycline detection with silver-lignin bio-spacer at attomolar sensitivity. *Plasmonics* 13, 955–960.
- Chen, J., Chen, Q., Chen, J., Qiu, H., 2016. Magnetic carbon nitride nanocomposites as enhanced peroxidase mimetics for use in colorimetric bioassays, and their application to the determination of H₂O₂ and glucose. *Microchim. Acta* 183, 3191–3199.
- Chen, X., Wu, G., Cai, Z., Oyama, M., Chen, X., 2014. Advances in enzyme-free electrochemical sensors for hydrogen peroxide, glucose, and uric acid. *Microchim. Acta* 181, 689–705.
- Chen, X., Ji, D., Wang, X., Zang, L., 2017. Review on nano zerovalent iron (nZVI): from modification to environmental applications. *IOP Conf. Ser.: Earth Environ. Sci.* 012004
- Choleva, T.G., Gatselou, V.A., Tsogas, G.Z., Giokas, D.L., 2018. Intrinsic peroxidase-like activity of rhodium nanoparticles, and their application to the colorimetric determination of hydrogen peroxide and glucose. *Microchim. Acta* 185, 22.
- Choleva, T.G., Gatselou, V.A., Tsogas, G.Z., Giokas, D.L., 2018. Intrinsic peroxidase-like activity of rhodium nanoparticles, and their application to the colorimetric determination of hydrogen peroxide and glucose. *Microchim. Acta* 185, 1–9.
- Daniel, M.-C., Astruc, D., 2004. Gold nanoparticles: assembly, supramolecular chemistry, quantum-size-related properties, and applications toward biology, catalysis, and nanotechnology. *Chem. Rev.* 104, 293–346.
- Ding, C., Yan, Y., Xiang, D., Zhang, C., Xian, Y., 2016. Magnetic Fe₃S₄ nanoparticles with peroxidase-like activity, and their use in a photometric enzymatic glucose assay. *Microchim. Acta* 183, 625–631.
- Favre, N., Ahmad, Y., Pierre, A.C., 2011. Biomaterials obtained by gelation of silica precursor with CO₂ saturated water containing a carbonic anhydrase enzyme. *J. Sol-Gel Sci. Technol.* 58, 442–451.
- Haddad Irani-nezhad, M., Khataee, A., Hassanzadeh, J., Orooji, Y., 2019. A chemiluminescent method for the detection of H₂O₂ and glucose based on intrinsic peroxidase-like activity of WS₂ quantum dots. *Molecules* 24, 689.
- Hasebe, Y., Eguchi, M., 2003. Chemical pollutant treatment by hydrogen peroxide with high reaction efficiency. *Jpn Kokai Tokkyo Koho An* 360884, 2003.

- He, Y., Niu, X., Shi, L., Zhao, H., Li, X., Zhang, W., et al, 2017. Photometric determination of free cholesterol via cholesterol oxidase and carbon nanotube supported Prussian blue as a peroxidase mimic. *Microchim. Acta* 184, 2181–2189.
- Hoyo, J., Ivanova, K., Torrent-Burgues, J., Tzanov, T., 2020. Interaction of silver-lignin nanoparticles with mammalian mimetic membranes. *Front. Bioeng. Biotechnol.* 8, 439.
- Jiang, Y., Miles, P., 1993. Generation of H₂O₂ during enzymic oxidation of catechin. *Phytochemistry* 33, 29–34.
- Kirkman, H.N., Gaetani, G.F., 2007. Mammalian catalase: a venerable enzyme with new mysteries. *Trends Biochem. Sci.* 32, 44–50.
- Lin, L., Song, X., Chen, Y., Rong, M., Zhao, T., Wang, Y., et al, 2015. Intrinsic peroxidase-like catalytic activity of nitrogen-doped graphene quantum dots and their application in the colorimetric detection of H₂O₂ and glucose. *Anal. Chim. Acta* 869, 89–95.
- Liu, H., Ma, H., Xu, H., Wen, J., Huang, Z., Qiu, Y., et al, 2019. Hollow and porous nickel sulfide nanocubes prepared from a metal-organic framework as an efficient enzyme mimic for colorimetric detection of hydrogen peroxide. *Anal. Bioanal. Chem.* 411, 129–137.
- Liu, S., Tian, J., Wang, L., Luo, Y., Sun, X., 2012. A general strategy for the production of photoluminescent carbon nitride dots from organic amines and their application as novel peroxidase-like catalysts for colorimetric detection of H₂O₂ and glucose. *RSC Adv.* 2, 411–413.
- Liu, Q., Yang, Y., Li, H., Zhu, R., Shao, Q., Yang, S., et al, 2015. NiO nanoparticles modified with 5, 10, 15, 20-tetrakis (4-carboxyl phenyl)-porphyrin: promising peroxidase mimetics for H₂O₂ and glucose detection. *Biosens. Bioelectron.* 64, 147–153.
- Lu, Y., Yu, J., Ye, W., Yao, X., Zhou, P., Zhang, H., et al, 2016. Spectrophotometric determination of mercury (II) ions based on their stimulation effect on the peroxidase-like activity of molybdenum disulfide nanosheets. *Microchim. Acta* 183, 2481–2489.
- Nakashima, K., Wada, M., Kuroda, N., Akiyama, S., Imai, K., 1994. High-performance liquid chromatographic determination of hydrogen peroxide with peroxyoxalate chemiluminescence detection. *J. Liq. Chromatogr. Relat. Technol.* 17, 2111–2126.
- Nguyen, N.D., Van Nguyen, T., Chu, A.D., Tran, H.V., Tran, L.T., Huynh, C.D., 2018. A label-free colorimetric sensor based on silver nanoparticles directed to hydrogen peroxide and glucose. *Arabian J. Chem.* 11, 1134–1143.
- Nishan, U., Bashir, F., Muhammad, N., Khan, N., Rahim, A., Shah, M., et al, 2019. Ionic liquid as a moderator for improved sensing properties of TiO₂ nanostructures for the detection of acetone biomarker in diabetes mellitus. *J. Mol. Liq.* 294, 111681.
- Nishan, U., Gul, R., Muhammad, N., Asad, M., Rahim, A., Shah, M., et al, 2020. Colorimetric based sensing of dopamine using ionic liquid functionalized drug mediated silver nanostructures. *Microchem. J.* 159, 105382.
- Nishan, U., Sabba, U., Rahim, A., Asad, M., Shah, M., Iqbal, A., et al, 2021. Ionic liquid tuned titanium dioxide nanostructures as an efficient colorimetric sensing platform for dopamine detection. *Mater. Chem. Phys.* 124289.
- Nossol, E., Zarbin, A.J., 2009. A simple and innovative route to prepare a novel carbon nanotube/prussian blue electrode and its utilization as a highly sensitive H₂O₂ amperometric sensor. *Adv. Funct. Mater.* 19, 3980–3986.
- Rogers, R.D., Seddon, K.R., 2003. Ionic liquids—solvents of the future? *Science* 302, 792–793.
- Salimi, A., Hallaj, R., Soltanian, S., Mamkhezri, H., 2007. Nanomolar detection of hydrogen peroxide on glassy carbon electrode modified with electrodeposited cobalt oxide nanoparticles. *Anal. Chim. Acta* 594, 24–31.
- Schmid, G., Talapin, D., Shevchenko, E., 2004. *Metal Nanoparticles*. Wiley-VCH, Weinheim, Germany, p. 328368.
- Shankar, S., Rhim, J.-W., 2017. Preparation and characterization of agar/lignin/silver nanoparticles composite films with ultraviolet light barrier and antibacterial properties. *Food Hydrocolloids* 71, 76–84.
- Shin, H.Y., Kim, B.-G., Cho, S., Lee, J., Na, H.B., Kim, M.I., 2017. Visual determination of hydrogen peroxide and glucose by exploiting the peroxidase-like activity of magnetic nanoparticles functionalized with a poly (ethylene glycol) derivative. *Microchim. Acta* 184, 2115–2122.
- Swaidan, A., Addad, A., Tahon, J.-F., Barras, A., Toufaily, J., Hamieh, T., et al, 2020. Ultrasmall CuS-BSA-Cu₃ (PO₄)₂ nanozyme for highly efficient colorimetric sensing of H₂O₂ and glucose in contact lens care solutions and human serum. *Anal. Chim. Acta*.
- Theyagarajan, K., Elanchezian, M., Aayushi, P.S., Thenmozhi, K., 2020. Facile strategy for immobilizing horseradish peroxidase on a novel acetate functionalized ionic liquid/MWCNT matrix for electrochemical biosensing. *Int. J. Biol. Macromol.* 163, 358–365.
- Tian, J., Liu, Q., Ge, C., Xing, Z., Asiri, A.M., Al-Youbi, A.O., et al, 2013. Ultrathin graphitic carbon nitride nanosheets: a low-cost, green, and highly efficient electrocatalyst toward the reduction of hydrogen peroxide and its glucose biosensing application. *Nanoscale* 5, 8921–8924.
- Tian, J., Liu, Q., Asiri, A.M., Qusti, A.H., Al-Youbi, A.O., Sun, X., 2013. Ultrathin graphitic carbon nitride nanosheets: a novel peroxidase mimetic, Fe doping-mediated catalytic performance enhancement and application to rapid, highly sensitive optical detection of glucose. *Nanoscale* 5, 11604–11609.
- Usui, Y., Sato, K., Tanaka, M., 2003. catalytic dihydroxylation of olefins with hydrogen peroxide: An organic-solvent-and metal-free system. *Angew. Chem. Int. Ed.* 42, 5623–5625.
- Velegarki, T., Poulos, I., Charalabaki, M., Kalogerakis, N., Samaras, P., Mantzavinos, D., 2006. Photocatalytic and sonolytic oxidation of acid orange 7 in aqueous solution. *Appl. Catal. B* 62, 159–168.
- Wang, X., Hao, J., 2016. Recent advances in ionic liquid-based electrochemical biosensors. *Sci. Bull.* 61, 1281–1295.
- Wang, B., Ju, P., Zhang, D., Han, X., Zheng, L., Yin, X., et al, 2016. Colorimetric detection of H₂O₂ using flower-like Fe₂ (MoO₄)₃ microparticles as a peroxidase mimic. *Microchim. Acta* 183, 3025–3033.
- Wang, N., Sun, J., Chen, L., Fan, H., Ai, S., 2015. A Cu₂ (OH)₃ Cl-CeO₂ nanocomposite with peroxidase-like activity, and its application to the determination of hydrogen peroxide, glucose and cholesterol. *Microchim. Acta* 182, 1733–1738.
- Wen, Z., Wang, Q., Li, J., 2008. Template synthesis of aligned carbon nanotube arrays using glucose as a carbon source: Pt decoration of inner and outer nanotube surfaces for fuel-cell catalysts. *Adv. Funct. Mater.* 18, 959–964.
- Xiang, Z., Wang, Y., Ju, P., Zhang, D., 2016. Optical determination of hydrogen peroxide by exploiting the peroxidase-like activity of AgVO₃ nanobelts. *Microchim. Acta* 183, 457–463.
- Xie, F., Cao, X., Qu, F., Asiri, A.M., Sun, X., 2018. Cobalt nitride nanowire array as an efficient electrochemical sensor for glucose and H₂O₂ detection. *Sens. Actuators, B* 255, 1254–1261.
- Zarif, F., Rauf, S., Qureshi, M.Z., Shah, N.S., Hayat, A., Muhammad, N., et al, 2018. Ionic liquid coated iron nanoparticles are promising peroxidase mimics for optical determination of H₂O₂. *Microchim. Acta* 185, 302.
- Zarif, F., Khurshid, S., Muhammad, N., Zahid Qureshi, M., Shah, N. S., 2020. Colorimetric Sensing of Hydrogen Peroxide Using Ionic-Liquid-Sensitized Zero-Valent Copper Nanoparticle (nZVCu). *ChemistrySelect* 5, 6066–6074.
- Zhan, T., Kang, J., Li, X., Pan, L., Li, G., Hou, W., 2018. NiFe layered double hydroxide nanosheets as an efficiently mimic enzyme for colorimetric determination of glucose and H₂O₂. *Sens. Actuators, B* 255, 2635–2642.
- Zhang, Q., Li, M., Guo, C., Jia, Z., Wan, G., Wang, S., et al, 2019. Fe₃O₄ Nanoparticles Loaded on Lignin Nanoparticles Applied as a Peroxidase Mimic for the Sensitively Colorimetric Detection of H₂O₂. *Nanomaterials* 9, 210.

- Zhang, Q., Chen, C., Wan, G., Lei, M., Chi, M., Wang, S., et al, 2019. Solar light induced synthesis of silver nanoparticles by using lignin as a reductant, and their application to ultrasensitive spectrophotometric determination of mercury (II). *Microchim. Acta* 186, 727.
- Zhang, W., Niu, X., Li, X., He, Y., Song, H., Peng, Y., et al, 2018. A smartphone-integrated ready-to-use paper-based sensor with mesoporous carbon-dispersed Pd nanoparticles as a highly active peroxidase mimic for H₂O₂ detection. *Sens. Actuators, B* 265, 412–420.
- Zhong, Y., Deng, C., He, Y., Ge, Y., Song, G., 2016. Exploring a monothiolated β -cyclodextrin as the template to synthesize copper nanoclusters with exceptionally increased peroxidase-like activity. *Microchim. Acta* 183, 2823–2830.